

H-WM: Robotic Task and Motion Planning Guided by Hierarchical World Model

Jinbang Huang^{1*}, Wenyuan Chen^{1,2*}, Zhiyuan Li^{1,2}, Oscar Pang^{1,2}, Xiao Hu¹, Lingfeng Zhang¹, Yuanzhao Hu^{1,3}, Zhanguang Zhang¹, Mark Coates⁴, Tongtong Cao¹, Xingyue Quan¹, Yingxue Zhang¹

Abstract—World models are becoming central to robotic planning and control as they enable prediction of future state transitions. Existing approaches often emphasize video generation or natural-language prediction, which are difficult to ground in robot actions and suffer from compounding errors over long horizons. Classic task and motion planning models world transition in logical space, enabling robot-executable and robust long-horizon reasoning. However, they typically operate independently of visual perception, preventing synchronized symbolic and visual state prediction. We propose a Hierarchical World Model (H-WM) that jointly predicts logical and visual state transitions within a unified framework. H-WM combines a high-level logical world model with a low-level visual world model, integrating the long-horizon robustness of symbolic reasoning with visual grounding. The hierarchical outputs provide stable intermediate guidance for long-horizon tasks, mitigating error accumulation and enabling robust execution across extended task sequences. Experiments across multiple vision–language–action (VLA) control policies demonstrate the effectiveness and generality of H-WM’s guidance.

I. INTRODUCTION

Recent advances in Vision–Language–Action (VLA) models have enabled robotic systems that tightly couple multi-modal perception and control via large pre-trained foundation models, achieving stronger generalization than traditional modular pipelines. However, most existing VLA methods adopt an end-to-end paradigm that maps visual observations and language instructions directly to low-level actions, resulting performance decrease on long-horizon tasks [1]. This failure is driven by compounding execution errors, ambiguous goal specifications, limited intermediate supervision, and overfitting to agent-centric representations.

A natural response to these limitations is to introduce richer intermediate guidance; however, existing approaches fall into three dominant paradigms, each with fundamental shortcomings. First, LLM-based hierarchical planners decompose tasks into subgoals or action sequences [2], but are fundamentally constrained by language as the intermediate interface: LLMs struggle to reason about physical constraints, and their vague, unstructured representations lead to semantic–execution misalignment [2, 3]. Second, world-model-based approaches aim to provide predictive visual guidance [4, 5], yet existing formulations suffer from complementary limitations, particularly in long-horizon settings

where compounding prediction errors degrade planning reliability. Third, classical Task and Motion Planning (TAMP) achieves long-horizon consistency through explicit logical world models for symbolic reasoning [6], but relies on manually designed abstractions and engineered perception-to-symbol pipelines that are weakly aligned with raw visual observations, resulting in brittleness to perception noise and poor scalability to unstructured environments [7]. Consequently, none of these paradigms delivers the informative, grounded, and long-horizon–robust guidance required for reliable VLA execution.

In this paper, we propose a novel hierarchical world model (H-WM) that jointly predicts logical and visual state transitions within a unified framework, enabling more effective intermediate guidance for VLA models on complex long-horizon tasks. First, we introduce a logical world model that performs long-horizon symbolic reasoning by predicting structured logical state transitions and action sequences, providing globally consistent task-level guidance while explicitly enforcing logical consistency and physical constraints. Second, we introduce a latent-feature–based visual world model conditioned on logical states and actions, which generates a sequence of latent visual subgoals to ground logical intermediate states into perceptual space. Together, the proposed hierarchical world model bridges high-level symbolic reasoning and low-level perceptual grounding, delivering informative, grounded, and long-horizon–robust guidance by combining the complementary strengths of prior approaches. To summarize, our key contributions are: (1) A hierarchical world model framework to align long-horizon logical transitions with visual dynamics for coherent future prediction and task execution. (2) A logical world model, implemented as a fine-tuned LLM that internalizes symbolic planning behaviors to provide structured and globally consistent guidance. (3) A visual world model to generate compact latent subgoal features conditioned on predicted logical states and future actions. (4) A systematic pipeline to integrate logical and visual guidance into VLA models, enabling physically grounded execution.

II. RELATED WORK

A. World Model

World models are powerful paradigms for robotics. Recent work has shown their effectiveness across a range of robotic settings, including policy learning [8, 9], policy evaluation [10, 11], test-time rollout simulation [12, 13],

¹Huawei Noah’s Ark Lab, ²University of Toronto, ³University of British Columbia, ⁴McGill University, *Equal contribution
Correspond to: jinbang.huang.work@gmail.com

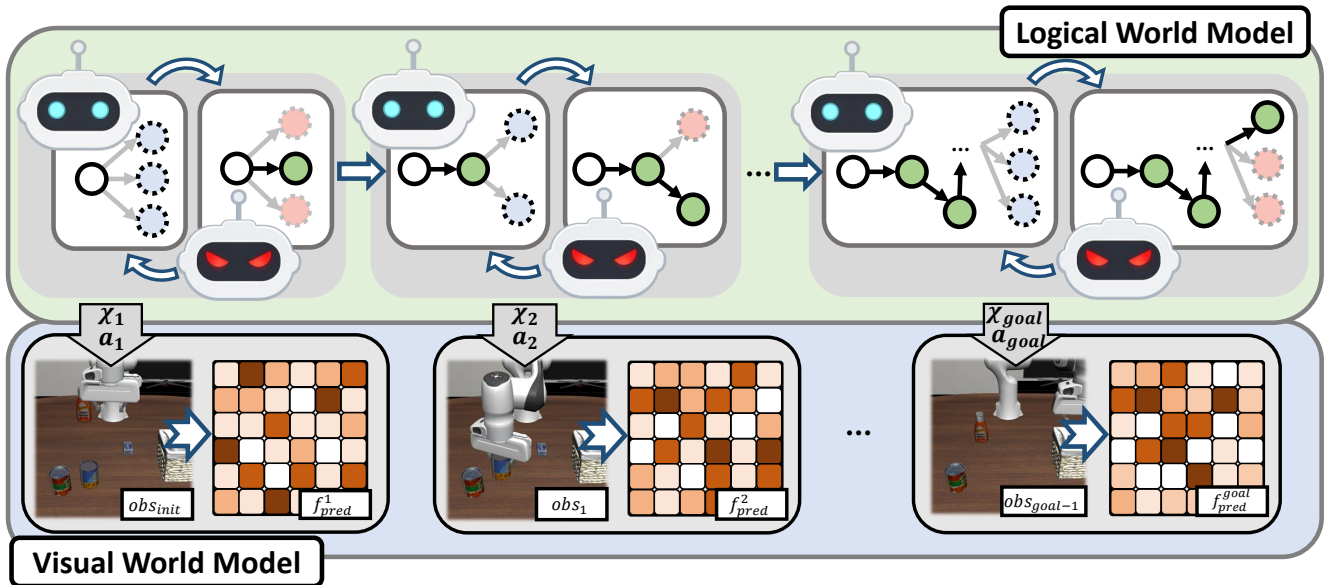


Fig. 1: Overall Framework: The proposed Hierarchical World Model jointly models transitions in both logical and visual latent spaces to guide robot policies. The logical world model iteratively searches and evaluates candidate actions and state transitions to produce a coherent sequence of actions and intermediate logical states. Conditioned on the current observation obs_m , the predicted action a_{m+1} , and the resulting logical state \mathcal{X}_{m+1} , the visual world model generates a latent visual subgoal feature f_{pred}^{m+1} . Together, obs_m , a_{m+1} , and f_{pred}^{m+1} serve as guidance for downstream robot control policies to enable reliable and physically feasible long-horizon execution.

and unified model-policy training [14–16]. World models enable reliable future reasoning and can generate large-scale multi-modal data [14–17]. Recent systems further demonstrate that world models can be directly adapted for action generation [18]. Most existing approaches focus on pixel-level world modeling, yet real-world dynamics can be captured at multiple abstraction levels. Lower-level representations offer high expressivity but suffer from poor sample efficiency and generalization [19, 20], whereas higher-level abstractions exhibit the opposite trade-off [21, 22]. Achieving a balance across levels remains an open challenge [23].

B. Vision-Language-Action Models

Vision-Language-Action (VLA) models enable direct mapping from visual observations and language instructions to robotic actions and have become a dominant paradigm for general-purpose robot control [24, 25]. End-to-end VLA models directly generate low-level actions from multi-modal inputs via large-scale pretraining [26–29], but suffer from performance degradation on long-horizon tasks due to goal ambiguity and error accumulation [1]. Hierarchical methods mitigate this issue by introducing intermediate guidance [4]. Prior work explores various guidance such as keypoints [30, 31], language [2], and visual predictions [3, 32]. While these approaches improve robot control, they remain vulnerable to error propagation and struggle with long-horizon tasks.

C. Task and Motion Planning

Task and motion planning (TAMP) integrates symbolic reasoning with motion generation to solve multi-step tasks

under physical constraints [6], but often suffers from limited scalability. To address this, prior work has explored imitation learning to accelerate planning [7, 33] and reinforcement learning to enhance adaptability in dynamic environments [34, 35]. More recently, LLM-based TAMP has leveraged language priors to guide planning [36–38]. Another line of work attempts to learn planning domains to improve scalability [39–46], but primarily focuses on abstract world modeling without visual grounding. A framework that jointly captures logical and visual dynamics to enable simultaneous prediction of logical transitions and visual observations remains lacking.

III. PRELIMINARY

A. Symbolic Formalization

A PDDL planning domain is defined as $\mathcal{D} = (\mathcal{P}, \mathcal{A})$, where \mathcal{P} is a finite set of predicate symbols and \mathcal{A} is a set of parameterized action schemas. For a given planning problem, let $\mathcal{O} = \{o_1, \dots, o_n\}$ denote the set of objects. Each **predicate** $p \in \mathcal{P}$ is associated with an arity k and defines a Boolean relation $p : \mathcal{O}^k \rightarrow \{0, 1\}$. Instantiating a predicate with concrete objects yields a *ground atom*. The set of all possible ground atoms is defined as $\mathcal{G} = \{p(o_1, \dots, o_k) \mid p \in \mathcal{P}, o_i \in \mathcal{O}\}$. A symbolic logical state is represented as a set of true ground atoms, $\mathcal{X} \subseteq \mathcal{G}$. An **action schema** $a \in \mathcal{A}$ is defined as $a = \langle \text{Pre}(a), \text{Add}(a), \text{Del}(a) \rangle$, where $\text{Pre}(a)$, $\text{Add}(a)$, and $\text{Del}(a)$ are sets of atoms denoting the preconditions, add effects, and delete effects, respectively. Binding an action schema a with a tuple of objects $(o_1, \dots, o_j) \in \mathcal{O}^j$ produces a *ground action* $a(o_1, \dots, o_j)$. A ground action is applicable in state \mathcal{X}^m if $\text{Pre}(a) \subseteq \mathcal{X}^m$. Executing

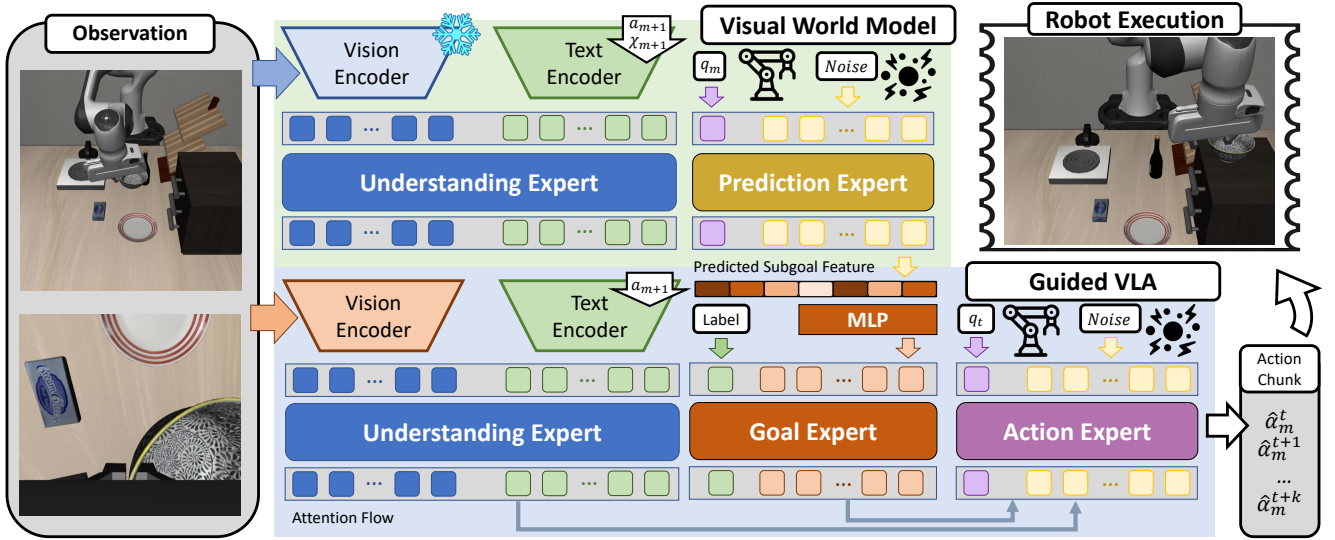


Fig. 2: Overview of the Visual World Model and VLA integration: The world model operates at a lower temporal frequency (once per subtask step m), while the VLA runs at a higher control frequency (each time step t). (a) The visual world model consists of an understanding expert that encodes the low-frequency observation obs_m , joint state q_m , logical action a_{m+1} , and predicted logical state \mathcal{X}_{m+1} , and a prediction expert that generates the sub-goal-state visual latent feature f_{pred}^{m+1} for downstream guidance. (b) The modified VLA includes an understanding expert that encodes the high-frequency observation obs_t , joint configuration q_t , and a_{m+1} , together with a goal expert that processes f_{pred}^{m+1} . The action expert attends to both understanding and goal experts to integrate current observations with goal constraints for motion generation.

an applicable ground action induces a deterministic state transition $\mathcal{X}^{m+1} = (\mathcal{X}^m \setminus \text{Del}(a)) \cup \text{Add}(a)$.

B. Sub-goal Visual Representation

We consider a long-horizon task decomposed into a sequence of subtasks in symbolic space, indexed by m . At subtask m , the robot observes an RGB image obs_m , receives the next logical action a_{m+1} describing the intended subtask, the resulting logical state \mathcal{X}_{m+1} , and joint configuration q_m . Let $\phi(\cdot)$ denote a fixed vision encoder that maps images into a d -dimensional latent space $\mathcal{F} \subset \mathbb{R}^d$. For any image g , its latent representation is defined as $f = \phi(g)$. For each subtask, we define a ground-truth subgoal image corresponding to successful completion, denoted as g_{goal}^{m+1} , with latent feature $f_{\text{goal}}^{m+1} = \phi(g_{\text{goal}}^{m+1})$. The visual world model predicts a latent goal feature $f_{\text{pred}}^{m+1} \in \mathcal{F}$ conditioned on the subtask state $(obs_m, a_{m+1}, \mathcal{X}_{m+1}, q_m)$.

IV. METHODOLOGY

Our framework operates at two temporal resolutions. For each subtask step m , the logical and visual world models are invoked once, whereas the VLA performs continuous low-level control across all time steps t within that subtask. Here, obs_m and q_m denote the observation and joint configuration at the start of subtask m , while obs_t and q_t represent the step-level observation and joint state at each control step.

A. Logic World Model

The logical world model enables long-horizon reasoning in symbolic space. Classical TAMP frameworks rely on hand-crafted PDDL domains to model logical transitions [6],

which are brittle under imperfect logical state estimation. To improve robustness, we learn symbolic planning dynamics directly from data using LLMs. We curate the training dataset by annotating each subtask m with logical states \mathcal{X}_m and actions a_m , aligned with observations obs_m and robot configurations q_m , forming unified representations $\langle \mathcal{X}_m, a_m, obs_m, q_m \rangle$. From each episode, we extract symbolic action sequences and corresponding logical state transitions, which are converted into chain-of-thought (CoT) explanations that explicitly describe logical transitions and goal progression following approaches in [47]. A base LLM is fine-tuned on these traces to learn symbolic transition dynamics, yielding a logical world model M_L .

As is shown in Fig. 1, during inference, M_L serves a dual role: as M_L^{search} , it proposes candidate logical actions and predicted state transitions; as M_L^{eval} , it scores partial trajectories based on logical consistency and goal alignment. This effectively treats the learned model as both world model and structured reward. As M_L is learned from data, the generalization ability of the base model allows it to model logical transitions even under incomplete logical state labels, mitigating the brittleness of planning domains.

B. Visual World Model

The visual world model provides stable visual guidance for long-horizon motion control by aligning symbolic state prediction with latent visual representations. Unlike prior world models that rely on unconstrained iterative generation, we predict latent visual features strictly constrained by future logical state transitions. By predicting only end-of-subtask visual representations, the model avoids costly sequential vi-

sual generation and avoids error propagation in long horizon.

As shown in Fig. 2, the visual world model comprises an understanding expert and a prediction expert that together map symbolic information to a visually grounded subgoal. At subtask step m , the understanding expert encodes the observation obs_m together with the logical action a_{m+1} and resulting logical state \mathcal{X}_{m+1} , producing a joint representation that explicitly associates the logical state transition with its visual context. Conditioned on this joint representation and the current robot configuration q_m , the prediction expert outputs a latent visual subgoal feature f_{pred}^{m+1} in a shared feature space. The prediction is implemented via an iterative denoising process. During training, supervision is constructed by synchronizing logical states, logical actions, and the corresponding terminal keyframes. The predicted feature f_{pred}^{m+1} is aligned with the ground-truth feature f_{goal}^{m+1} , obtained by encoding the goal image with the same frozen vision encoder. Alignment is optimized using the sliced Wasserstein loss [48] to encourage distributional consistency and stable training. At inference time, the visual world model is queried once per subtask, and the predicted latent goal feature is kept fixed during its execution.

C. Hierarchical World Model Guidance for VLA

The guided VLA operates as low-level robot motion policy within our framework. Rather than acting solely conditioned on current observation, it utilizes structured guidance from both the logical and visual world models. The hierarchical information at multiple abstraction level enables the VLA to maintain consistency with long-horizon task structure while remaining responsive to local visual feedback.

As illustrated in Fig. 2, the sub-goal VLA consists of three experts: an understanding expert, a goal expert, and an action expert. Given the current observation obs_t and logical action a_{m+1} , the understanding expert encodes visual inputs and fuses them with logical information to form a multi-modal representation of the current scene. In parallel, the goal expert receives the latent visual latent features f_{pred}^{m+1} representing the desired visual outcome. The action expert then conditions jointly on obs_t , a_{m+1} , f_{pred}^{m+1} and current joint configuration q_t to generate a sequence of low-level action chunks containing k steps $\hat{\alpha}_m^{t:t+k}$. All experts are implemented as decoder-only transformer [49] initialized from PaliGemma [50]. To integrate world-model guidance into action generation, we introduce cross-attention mechanism in which the action expert attends to both understanding and goal experts. Reverse information flow is explicitly disallowed to preserve hierarchical structure and stabilize training. The policy is trained end-to-end using a flow-matching objective [51].

D. Subtask Completion and Transition Prediction

The decomposed sequential subtasks require detection of subtask transitions. We introduce a subtask completion predictor head to monitor execution progress and signals when the current subtask a_{m+1} is achieved. Built upon the understanding expert, the predictor takes the observation at

the same frequency as VLA, obs_t , and logical action a_{m+1} as input. A dedicated [CLS] token, is fed to a lightweight classification head to determine subtask completion, enabling stable and synchronized transitions within the hierarchical pipeline. During inference, the completion predictor head is queried at every step for smooth subtask transition.

V. EXPERIMENTS

A. Training Dataset

We train our hierarchical world model on two datasets: a logically synchronized version of LIBERO [52] and the RoboCerebra [53] benchmark. For LIBERO, we construct a logically synchronized variant based on the standard LIBERO dataset. The resulting dataset provides frame-level alignment between robot states, visual observations, logical states, and logical actions, enabling joint training of the logical and visual world models. Annotations are obtained through a two-stage labeling process. First, we replay each episode and apply a set of pre-designed predicate classifiers to infer logical states and actions at every timestep. Second, we manually screen the labeled data to correct annotation errors. For RoboCerebra, we directly adopt the provided task decompositions and unify the logical actions and predicates across all tasks to maintain a consistent representation.

B. Benchmark and Evaluation

We evaluate H-WM alongside a range of VLA baselines across diverse long-horizon planning and control benchmarks, including LIBERO-10 [52], RoboCerebra [53], and LIBERO-LoHo. We introduce **LIBERO-LoHo** as a more challenging long-horizon benchmark derived from the standard LIBERO benchmark. LIBERO-LoHo comprises five long-horizon tasks constructed by approximately doubling the task horizon of the original LIBERO tasks through increasing the number of manipulated objects and dependencies. Specifically, **Task 1** is a five-step task that requires placing the front butter and the chocolate pudding into the top drawer of the wooden cabinet, followed by closing the drawer. **Task 2** is a six-step task that requires placing the alphabet soup, the butter, and the tomato sauce into the basket. **Task 3** is a six-step task in which the robot places the alphabet soup, the cream cheese, and the butter into the wooden tray. **Task 4** is a six-step task that involves placing the black bowl on the left, the salad dressing, and the chocolate pudding into the wooden tray. **Task 5** is a seven-step task that requires placing the butter at the back and the chocolate pudding into the top drawer of the cabinet, closing the drawer, and then placing the black bowl on top of the cabinet. The task horizons in LIBERO-LoHo are significantly longer than those in the original LIBERO benchmark (1–3 steps), enabling a more rigorous evaluation of policy performance under long-horizon challenges. Performance is primarily measured by **Success Rate**, defined as the percentage of tasks successfully completed. For extra-long horizon benchmarks, including LIBERO-LoHo (*up to 7 steps*) and RoboCerebra (*up to 20 steps*), where full completion remains challenging for most methods, we also

TABLE I: Performance on the LIBERO-LoHo benchmark. For each task, we report Q-Score and Success Rate (in %). The best results are shown in **bold**, and the second-best results are underlined.

Methods	Tasks Q-score / Task Success Rate					
	Task 1	Task 2	Task 3	Task 4	Task 5	Average
H-WM- $\pi_{0.5}$ (ours)	98.0/94.0	86.7/60.0	74.0/46.0	<u>70.7/42.0</u>	95.0/82.0	84.9/64.8
H-WM-Stable-Diffusion- $\pi_{0.5}$	92.7/82.0	80.0/46.0	65.3/30.0	74.0/34.0	<u>93.5/80.0</u>	81.1/54.4
Logic-guided $\pi_{0.5}$	<u>95.3/86.0</u>	<u>84.7/58.0</u>	54.7/16.0	39.3/4.0	92.0/78.0	73.2/48.4
LLM-guided $\pi_{0.5}$	84.7/54.0	80.7/42.0	<u>68.0/24.0</u>	41.3/4.0	59.5/10.0	66.8/26.8
$\pi_{0.5}$	66.0/4.0	73.3/24.0	54.7/4.0	44.7/0.0	38.0/0.0	55.3/6.4
π_0	54.0/0.0	62.0/28.0	44.0/0.0	31.3/0.0	34.0/0.0	45.1/5.6
X-VLA	48.8/0.0	16.7/0.0	23.3/0.0	33.3/0.0	40.0/0.0	32.4/0.0
Gr00t-N1.5	0.0/0.0	30.7/0.0	34.7/0.0	2.7/0.0	0.0/0.0	13.6/0.0
OpenVLA-OFT	0.0/0.0	60.0/0.0	17.3/0.0	22.7/0.0	0.0/0.0	20.0/0.0
OpenVLA	0.0/0.0	2.7/0.0	24.0/0.0	2.7/0.0	0.0/0.0	5.9/0.0

report **Q-Score**, defined as the fraction of completed sub-goals over the total number of sub-goals. Q-Score provides a more informative evaluation on the task progress.

C. Baselines

We evaluate the effectiveness of H-WM guidance for VLAs and compare against a diverse set of baseline models, including SOTA VLA approaches as π_0 [28], $\pi_{0.5}$ [29], OpenVLA [27], OpenVLA(OFT) [54], X-VLA [55], and GR00T [56]. We also include a hierarchical planning baseline that use a natural-language-based task decomposition with VLA-based motion execution [2] together with $\pi_{0.5}$, indicated as LLM-guided $\pi_{0.5}$. By these comparisons, we aim to show the advantages of H-WM in providing effective intermediate guidance for VLAs on long-horizon tasks.

D. Implementation

For LIBERO-10 and LIBERO-LoHo, all VLA models are trained on the LIBERO dataset. For RoboCerebra, the models are trained on the provided training split and evaluated on the ideal test set. We follow the standard training configuration for $\pi_{0.5}$, adopting a learning rate of $5e-5$ over 60k training steps, implemented in PyTorch. Baseline methods use publicly released LIBERO fine-tuned checkpoints. The visual world model is initialized from PaliGemma [50] and extended with a prediction head composed of two fully connected layers, mapping feature representations from 2048 to 4096 dimensions and back to 2048 dimensions. It uses the same training hyperparameters as the VLA models but is trained for 100k steps. The visual encoder used is SigLIP [57]. The logical world model is initialized from Qwen3-4B-Instruct and apply LoRA [58] fine-tuning for 10k steps with a learning rate of $1e-5$. Logical state estimations from visual observations are performed using an off-the-shelf VLM, Qwen3-VL-2B prompted with one-shot examples.

E. Ablation Studies

To validate the contribution of visual guidance beyond logical reasoning, we conduct a controlled ablation, Logic- $\pi_{0.5}$, in which visual world model is removed and only logical world model is retained. In addition, we vary the

visual guidance prediction mechanism by replacing latent visual feature prediction with pixel-level image generation based on Stable Diffusion [59]. This comparison allows us to examine whether latent representation prediction provides more effective visual guidance than image-generation.

VI. RESULTS

Our experiments aims to answer the following questions: (1) Does H-WM provide effective guidance for downstream VLAs? (2) How does the H-WM-guided VLA compare to baseline approaches and models? (3) How does each level of the world model contribute to the final performance? (4) Is the H-WM framework deployable in real-robot settings?

(1) Effectiveness of H-WM guidance: The results demonstrate that H-WM provides stable and effective guidance for long-horizon tasks across three benchmarks. On LIBERO-LoHo (Table I), H-WM-guided $\pi_{0.5}$ significantly outperforms $\pi_{0.5}$, improving success rate by over 50% and Q-score by near 30%. Similar gains are observed on RoboCerebra (Fig. 3.b), with improvements exceeding 10% in Q-score and nearly 10% in success rate. In contrast, $\pi_{0.5}$ attains relatively high Q-Scores but low Success Rates, often due to missing intermediate steps, ignored instructions, and incorrect action ordering, leading to partial completion but overall failure. On LIBERO-10 (Fig. 3.a), H-WM guidance still improves performance, though the margin is smaller. This is because LIBERO-10 tasks are much shorter, allowing VLAs to learn the full procedure without guidance.

(2) Comparison to Baselines: H-WM-guided $\pi_{0.5}$ consistently outperforms all baselines on long-horizon tasks (Table I, Fig. 3.b). Raw VLAs struggle with long-range dependencies, frequently omitting intermediate steps or misordering actions. In contrast, hierarchical guidance from H-WM ensures stable, globally consistent execution. Baseline VLAs are also sensitive to prompt variation, leading to incomplete task execution. While LLM-based language decomposition improves performance by splitting tasks into subtasks, LLM-guided $\pi_{0.5}$ still underperforms compared to both H-WM-guided and Logic-guided variants. This gap stems from the fact that natural language is inherently ambiguous and less structured than symbolic logic, and less grounded than

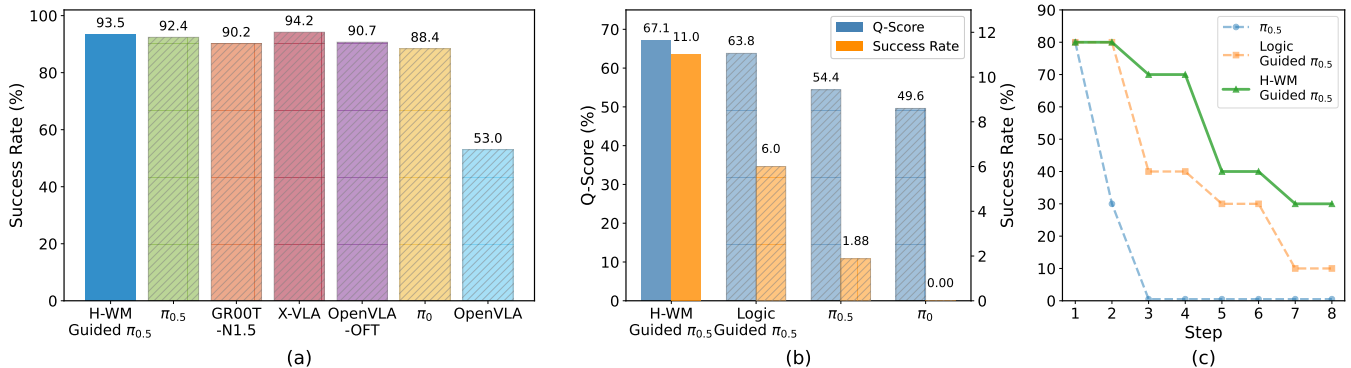


Fig. 3: (a) Evaluation results of H-WM-guided $\pi_{0.5}$ and various VLA baselines on the LIBERO-10 benchmark. (b) Evaluation results of H-WM-guided $\pi_{0.5}$ and baseline methods on the RoboCerebra benchmark. (c) Step-wise success rates in real-robot experiments. Solid colors indicate our method, whereas shaded bars or dashed lines denote baselines.

visual representations. By integrating logical reasoning with latent visual subgoals, H-WM delivers more reliable and robust guidance for long-horizon planning and control. On LIBERO-10 (Fig. 3.a), H-WM shows smaller gains and ranks second overall due to the shorter task horizons.

(3) Ablation Study: The ablation results further validate the necessity of bilevel guidance. As shown in Table I, logic-only guidance already surpasses the unguided baseline by over 40% in success rate and 15% in Q-score. Incorporating visual guidance yields consistent additional gains, providing more than 10% further improvement in Q-score and 17% in success rate. This confirms that visual world modeling provides actionable grounding for symbolic plans, improving alignment between symbolic constraints and perceptual execution. The results on RoboCerebra (Fig. 3.b) support the same conclusion. Moreover, the results show that pixel-level image generation is less effective than latent visual features. The H-WM-Stable-Diffusion- $\pi_{0.5}$ variant replaces latent visual prediction with Stable Diffusion-based image generation, yet achieves smaller performance gains than the default H-WM, exhibiting over a 10% drop in overall success rate. This is likely because pixel-level generation introduces unnecessary visual details and reconstruction noise, whereas latent features provide more compact guidance for VLAs.

(4) Real-World Experiment: To validate H-WM in the real world, we deploy it on a UR5e robot to perform an 8-step table-cleaning task (Fig. 4). The task involves setting up an office table with multiple object manipulations, requiring intensive spatial reasoning and long-horizon planning consistency. We compare step-wise success rate for π_0 , $\pi_{0.5}$, and H-WM- $\pi_{0.5}$. All models are trained on 40 manually collected trajectories. The robot is controlled via the UR5e control API with RealSense camera for visual input. As shown in Fig. 3.c, logical guidance substantially improves long-horizon success, while additional visual guidance further enhances performance with more accurate poses generation.

VII. CONCLUSION

We propose a hierarchical world model (H-WM) that jointly models logical and visual world dynamics to provide bilevel guidance for VLA models in long-horizon robotic

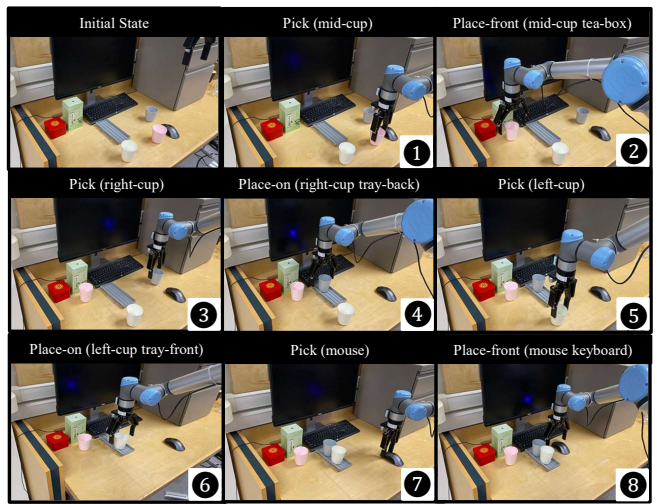


Fig. 4: Real-world experiment with UR5e robot evaluating H-WM guided $\pi_{0.5}$ on long-horizon manipulation task.

tasks. The logical world model captures global task structure and long-term dependencies, while the visual level grounds logical transitions into visually meaningful latent subgoals, enabling stable guidance of VLAs over extended horizons. Experimental results show that H-WM significantly improves long-horizon performance over base VLA models and hierarchical or end-to-end approaches. These findings demonstrate that hierarchical world modeling offers an effective and scalable guidance for bridging symbolic reasoning and perceptual grounding in VLA systems. Although the proposed Hierarchical World Model demonstrates strong performance in guiding long-horizon manipulation tasks, several limitations remain. First, H-WM introduces additional model components and training stages, leading to increased training cost and system complexity. Second, the logical world model depends on structured logical state representations, which assume that the task can be meaningfully formulated in a symbolic logical space. Future directions include enhancing training efficiency, reducing the need for explicit logical supervision, extending the framework to additional sensory modalities for improved spatial reasoning.

REFERENCES

- [1] Y. Yang, J. Sun, S. Kou, Y. Wang, and Z. Deng, “Lohovla: A unified vision-language-action model for long-horizon embodied tasks,” *arXiv preprint arXiv:2506.00411*, 2025.
- [2] L. X. Shi et al., “Hi robot: Open-ended instruction following with hierarchical vision-language-action models,” *arXiv preprint arXiv:2502.19417*, 2025.
- [3] H. Chen et al., “Goal-vla: Image-generative vlms as object-centric world models empowering zero-shot robot manipulation,” *arXiv preprint arXiv:2506.23919*, 2025.
- [4] R. Shao et al., “Large vlm-based vision-language-action models for robotic manipulation: A survey,” *arXiv preprint arXiv:2508.13073*, 2025.
- [5] J. Xiang et al., “Pan: A world model for general, interactable, and long-horizon world simulation,” *arXiv preprint arXiv:2511.09057*, 2025.
- [6] L. P. Kaelbling and T. Lozano-Pérez, “Hierarchical task and motion planning in the now,” in *2011 IEEE international conference on robotics and automation*, 2011.
- [7] T. Silver, R. Chitnis, A. Curtis, J. B. Tenenbaum, T. Lozano-Pérez, and L. P. Kaelbling, “Planning with learned object importance in large problem instances using graph neural networks,” in *Proceedings of the AAAI conference on artificial intelligence*, 2021.
- [8] D. Hafner, W. Yan, and T. Lillicrap, “Training agents inside of scalable world models,” *arXiv preprint arXiv:2509.24527*, 2025.
- [9] S. Li, Y. Gao, D. Sadigh, and S. Song, “Unified video action model,” *arXiv preprint arXiv:2503.00200*, 2025.
- [10] J. Quevedo, A. K. Sharma, Y. Sun, V. Suryavanshi, P. Liang, and S. Yang, “Worldgym: World model as an environment for policy evaluation,” *arXiv preprint arXiv:2506.00613*, 2025.
- [11] Y. Li, Y. Zhu, J. Wen, C. Shen, and Y. Xu, “Worldval: World model as real-world robot policies evaluator,” *arXiv preprint arXiv:2505.19017*, 2025.
- [12] A. Bar, G. Zhou, D. Tran, T. Darrell, and Y. LeCun, “Navigation world models,” in *Proceedings of the Computer Vision and Pattern Recognition Conference*, 2025.
- [13] Y. Yang et al., “Mindjourney: Test-time scaling with world models for spatial reasoning,” *arXiv preprint arXiv:2507.12508*, 2025.
- [14] Q. Zhao et al., “Cot-vla: Visual chain-of-thought reasoning for vision-language-action models,” in *Proceedings of the Computer Vision and Pattern Recognition Conference*, 2025.
- [15] H. Bi et al., “Motus: A unified latent action world model,” *arXiv preprint arXiv:2512.13030*, 2025.
- [16] W. Zhang et al., “Dreamvla: A vision-language-action model dreamed with comprehensive world knowledge,” *arXiv preprint arXiv:2507.04447*, 2025.
- [17] Y. Liao et al., “Genie envisioner: A unified world foundation platform for robotic manipulation,” *arXiv preprint arXiv:2508.05635*, 2025.
- [18] M. J. Kim et al., “Cosmos policy: Fine-tuning video models for visuomotor control and planning,” in *The Fourteenth International Conference on Learning Representations*, 2026.
- [19] A. Xie, F. Ebert, S. Levine, and C. Finn, “Improvisation through physical understanding: Using novel objects as tools with visual foresight,” *arXiv preprint arXiv:1904.05538*, 2019.
- [20] R. Hoque et al., “Visuospatial foresight for physical sequential fabric manipulation,” *Autonomous Robots*, 2022.
- [21] L. Manuelli, Y. Li, P. Florence, and R. Tedrake, “Keypoints into the future: Self-supervised correspondence in model-based reinforcement learning,” *arXiv preprint arXiv:2009.05085*, 2020.
- [22] D. Driess et al., “Palm-e: An embodied multimodal language model,” *arXiv preprint arXiv:2303.03378*, 2023.
- [23] E. Xing, M. Deng, J. Hou, and Z. Hu, “Critiques of world models,” *arXiv preprint arXiv:2507.05169*, 2025.
- [24] Y. Ma, Z. Song, Y. Zhuang, J. Hao, and I. King, “A survey on vision-language-action models for embodied ai,” *arXiv preprint arXiv:2405.14093*, 2024.
- [25] Y. Zhong et al., “A survey on vision-language-action models: An action tokenization perspective,” *arXiv preprint arXiv:2507.01925*, 2025.
- [26] B. Zitkovich et al., “Rt-2: Vision-language-action models transfer web knowledge to robotic control,” in *Conference on Robot Learning*, 2023.
- [27] M. J. Kim et al., “OpenVLA: An open-source vision-language-action model,” in *8th Annual Conference on Robot Learning*, 2024.
- [28] K. Black et al., “ π_0 : A vision-language-action flow model for general robot control,” *arXiv preprint arXiv:2410.24164*, 2024.
- [29] K. Black et al., “ $\pi_{0.5}$: A vision-language-action model with open-world generalization,” in *9th Annual Conference on Robot Learning*, 2025.
- [30] Z. Wu, Y. Zhou, X. Xu, Z. Wang, and H. Yan, “Momanipvla: Transferring vision-language-action models for general mobile manipulation,” in *Proceedings of the Computer Vision and Pattern Recognition Conference*, 2025.
- [31] W. Yuan et al., “Robopoint: A vision-language model for spatial affordance prediction for robotics,” *arXiv preprint arXiv:2406.10721*, 2024.
- [32] H. Zhen et al., “3d-vla: A 3d vision-language-action generative world model,” *arXiv preprint arXiv:2403.09631*, 2024.
- [33] M. Dalal, A. Mandlekar, C. Garrett, A. Handa, R. Salakhutdinov, and D. Fox, “Imitating task and motion planning with visuomotor transformers,” *arXiv preprint arXiv:2305.16309*, 2023.

- [34] R. Chitnis et al., “Guided search for task and motion plans using learned heuristics,” in *2016 IEEE International Conference on Robotics and Automation (ICRA)*, 2016.
- [35] C. Paxton, V. Raman, G. D. Hager, and M. Kobilarov, “Combining neural networks and tree search for task and motion planning in challenging environments,” in *2017 IEEE/RSJ International Conference on Intelligent Robots and Systems (IROS)*, 2017.
- [36] W. Huang et al., “Inner monologue: Embodied reasoning through planning with language models,” *arXiv preprint arXiv:2207.05608*, 2022.
- [37] S. Wang et al., “Llm³: Large language model-based task and motion planning with motion failure reasoning,” in *2024 IEEE/RSJ international conference on intelligent robots and systems (IROS)*, 2024.
- [38] Y. Chen, J. Arkin, Y. Hao, Y. Zhang, N. Roy, and C. Fan, “Prompt optimization in multi-step tasks (promst): Integrating human feedback and heuristic-based sampling,” in *Proceedings of the 2024 Conference on Empirical Methods in Natural Language Processing*, 2024.
- [39] M. Diehl, C. Paxton, and K. Ramirez-Amaro, “Automated generation of robotic planning domains from observations,” in *2021 IEEE/RSJ International Conference on Intelligent Robots and Systems (IROS)*, 2021.
- [40] N. Kumar, W. McClinton, R. Chitnis, T. Silver, T. Lozano-Pérez, and L. P. Kaelbling, “Learning efficient abstract planning models that choose what to predict,” in *Conference on Robot Learning*, 2023.
- [41] T. Silver et al., “Predicate invention for bilevel planning,” in *Proceedings of the AAAI Conference on Artificial Intelligence*, 2023.
- [42] Y. Liang et al., “Visualpredicator: Learning abstract world models with neuro-symbolic predicates for robot planning,” *arXiv preprint arXiv:2410.23156*, 2024.
- [43] J. Mao, T. Lozano-Pérez, J. B. Tenenbaum, and L. P. Kaelbling, “Learning reusable manipulation strategies,” in *Conference on Robot Learning*, 2023.
- [44] J. Huang, A. Tao, R. Marco, M. Bogdanovic, J. Kelly, and F. Shkurti, “Automated planning domain inference for task and motion planning,” in *2025 IEEE International Conference on Robotics and Automation (ICRA)*, 2025.
- [45] J. Huang, Y. Xiao, Z. Zhang, M. Coates, J. HAO, and Y. Zhang, “One demo is all it takes: Planning domain derivation with LLMs from a single demonstration,” in *The Fourteenth International Conference on Learning Representations*, 2026.
- [46] M. Han, Y. Zhu, S.-C. Zhu, Y. N. Wu, and Y. Zhu, “Interpret: Interactive predicate learning from language feedback for generalizable task planning,” in *Robotics: Science and Systems (RSS)*, 2024.
- [47] J. Huang et al., “Self-CriTeach: LLM self-teaching and self-critiquing for improving robotic planning via automated domain generation,” *arXiv preprint arXiv:2509.21543*, 2025.
- [48] E. Tanguy, R. Flamary, and J. Delon, “Properties of discrete sliced wasserstein losses,” *Mathematics of Computation*, 2025.
- [49] G. Team et al., “Gemma: Open models based on gemini research and technology,” *arXiv preprint arXiv:2403.08295*, 2024.
- [50] L. Beyer et al., “Paligemma: A versatile 3b vlm for transfer,” *arXiv preprint arXiv:2407.07726*, 2024.
- [51] Y. Lipman, R. T. Chen, H. Ben-Hamu, M. Nickel, and M. Le, “Flow matching for generative modeling,” *arXiv preprint arXiv:2210.02747*, 2022.
- [52] B. Liu et al., “Libero: Benchmarking knowledge transfer for lifelong robot learning,” *Advances in Neural Information Processing Systems*, 2023.
- [53] S. Han et al., “Robocerebra: A large-scale benchmark for long-horizon robotic manipulation evaluation,” in *The Thirty-ninth Annual Conference on Neural Information Processing Systems Datasets and Benchmarks Track*, 2025.
- [54] M. J. Kim, C. Finn, and P. Liang, “Fine-tuning vision-language-action models: Optimizing speed and success,” *arXiv preprint arXiv:2502.19645*, 2025.
- [55] J. Zheng et al., “X-VLA: Soft-prompted transformer as scalable cross-embodiment vision-language-action model,” in *The Fourteenth International Conference on Learning Representations*, 2026.
- [56] J. Bjorck et al., “Gr00t n1: An open foundation model for generalist humanoid robots,” *arXiv preprint arXiv:2503.14734*, 2025.
- [57] X. Zhai, B. Mustafa, A. Kolesnikov, and L. Beyer, “Sigmoid loss for language image pre-training,” in *Proceedings of the IEEE/CVF international conference on computer vision*, 2023.
- [58] E. J. Hu et al., “LoRA: Low-rank adaptation of large language models,” in *International Conference on Learning Representations*, 2022.
- [59] R. Rombach, A. Blattmann, D. Lorenz, P. Esser, and B. Ommer, “High-resolution image synthesis with latent diffusion models,” in *Proceedings of the IEEE/CVF conference on computer vision and pattern recognition*, 2022.